



Published in final edited form as:

J Mol Biol. 2007 June 1; 369(2): 419–428.

Sequence Determinants of E2-E6AP Binding Affinity and Specificity

Ziad M Eletr¹ and Brian Kuhlman^{1,*}

*1*Department of Biochemistry and Biophysics, University of North Carolina, Chapel Hill, NC 27599-7260, USA

Abstract

The conjugation of ubiquitin to substrates requires a series of enzymatic reactions consisting of an activating enzyme (E1), conjugating enzymes (E2) and ligases (E3). Tagging the appropriate substrate with ubiquitin is achieved by specific E2-E3 and E3-substrate interactions. E6AP, a member of the HECT family of E3s, has been previously shown to bind and function with the E2s UbcH7 and UbcH8. To decipher the sequence determinants of this specificity we have developed a quantitative E2-E3 binding assay based on fluorescence polarization and used this assay to measure the affinity of wild type and mutant E2-E6AP interactions. Alanine scanning of the E6AP-UbcH7 binding interface identified 4 side chains on UbcH7 and 6 side chains on E6AP that contribute more than 1 kcal/mol to the binding free energy. Two of the hot spot residues from UbcH7 (K96 and K100) are conserved in UbcH8 but vary across other E2s. To determine if these are key specificity determining residues, we attempted to induce a tighter association between the E2 UbcH5b and E6AP by mutating the corresponding positions in UbcH5b to lysines. Surprisingly, the mutations had little effect, but rather a mutation at UbcH7 position 4, which is not at a hot spot on the UbcH7-E6AP interface, significantly strengthened UbcH5b's affinity for E6AP. This result indicates that E2-E3 binding specificities are a function of both favorable interactions that promote binding, and unfavorable interactions that prevent binding with unwanted partners.

Keywords

Ubiquitin; UbcH7; E6AP; HECT; E2-E3 Specificity

Introduction

Protein ubiquitination is an essential eukaryotic pathway that influences nearly all cellular processes¹. The conjugation of ubiquitin to a protein substrate requires a cascade of enzymatic reactions beginning with the ubiquitin activating enzyme (E1). The E1 uses ATP to form a thioester bond between the carboxyl-terminus of ubiquitin and the E1 active site cysteine. The E1 then binds a ubiquitin conjugating enzyme (E2) and transfers ubiquitin to the E2 active site cysteine. The next step in the pathway requires a ubiquitin ligase (E3) which utilizes distinct domains to bind both E2 and substrate. The two major classes of E3s bind E2s using either a RING (*really interesting gene*) domain or a HECT (*homology to E6AP carboxy terminus*) domain. E3s containing a HECT domain form a third thioester intermediate with ubiquitin prior to transfer to substrate². E3s that contain a RING domain do not form a covalent

*Corresponding Author

Publisher's Disclaimer: This is a PDF file of an unedited manuscript that has been accepted for publication. As a service to our customers we are providing this early version of the manuscript. The manuscript will undergo copyediting, typesetting, and review of the resulting proof before it is published in its final citable form. Please note that during the production process errors may be discovered which could affect the content, and all legal disclaimers that apply to the journal pertain.

intermediate with ubiquitin, but rather bring the substrate in proximity of the E2 whereby transfer of ubiquitin proceeds directly from E2 to substrate.

The importance of specific E3-substrate interactions is apparent as aberrations can lead to improper substrate regulation and severe physiological consequences^{3; 4}. Often overlooked is the specificity of E2-E3 interactions as similar outcomes could potentially arise. The hierarchical nature of the ubiquitin pathway presents a formidable task in dissecting all E2-E3 and E3-substrate interactions. For example in humans there is a single E1, ~30 E2s and hundreds of potential E3s. In general, a given E2 will interact with multiple E3s while E3s only function with a limited subset of E2s⁴. Additionally, a given E3 may have more than one substrate and some substrates can be recognized by multiple E3s⁴. One possible method to dissect the network of interactions is to design altered specificity E2-E3 pairs that will function together but not with their wild type partners. Such an approach has been taken by Marc Timmers and colleagues who used a charge swap interaction across the UbcH5b-cNOT4 interface to create an altered specificity E2-RING pair⁵. The Timmers study, as well as others, have helped map the determinants of E2-RING specificity^{5; 6; 7; 8; 9}. Here, we examine the sequence determinants of E2-HECT specificity. In particular, we focus on the HECT domain protein, E6AP.

E6AP is the founding member of the HECT domain class of E3s. It was first identified as a protein that cooperates with the E6 protein from oncogenic forms of the human papillomavirus to down regulate the p53 tumor suppressor¹⁰. The conserved ~350 amino acid HECT domain adopts a bilobal structure and is always found at the C-terminus of E3s. A three residue hinge connects the N-terminal, E2 binding lobe with the catalytic C-terminal lobe and the interface created by the two lobes forms a highly conserved cleft containing the catalytic cysteine¹¹ (Figure 1(a)). Three crystal structures of HECT domains have revealed significantly different orientations of the two lobes implying conformational changes are necessary for catalysis^{11; 12; 13}. Hinge mutations to proline that restrict the conformational flexibility of the HECT domain result in impaired E3 activity¹². Also, some patients with Angelman syndrome (AS), a severe neurological disorder linked to E6AP, have acquired mutations within the conserved cleft which have been shown to reduce E6AP ligase activity^{14; 15}. Despite the significant progress on AS associated E6AP mutations, none of the identified E6AP substrates have been directly linked to the disorder¹⁶. A better understanding of HECT domains as well as their E2s and substrates may help combat such E3 associated diseases.

All E2 enzymes possess a conserved catalytic core domain of approximately 150 amino acids though some E2s also contain N- and C-terminal extensions which serve diverse functions¹⁶. The E2 core domain contains the residues responsible for catalysis as well as binding E1 and E3s. Crystal structures of the E2 UbcH7 bound to a HECT E3, E6AP¹¹, and a RING E3, c-Cbl¹⁷, revealed that E2s utilize similar residues to bind both classes of E3s. The majority of E3 binding residues are contained within the N-terminal helix (helix 1) as well as loops 4 and 7^{11; 17} (Figure 1(b)). In both E2-E3 structures, the primary contact at the interface arises from F63 on loop 4 of UbcH7 which is buried in a hydrophobic groove created by the E3^{11; 17}. This phenylalanine is present in all E2s that have been shown to function with HECT E3s^{11; 18}. The sequences of helix 1 and loop 7 of HECT binding E2s are more varied, and it has been proposed that these regions of the interface determine which HECT domains an E2 will bind¹¹. HECT E3s have been shown to form selective interactions with at least 3 distinct E2 subfamilies^{19; 20; 21; 22}. To decipher the sequence determinants of E2-E6AP specificity, we have performed a variety of mutagenesis experiments to map out which E2 and E6AP residues are important for E2-E6AP affinity, and have used this information along with multiple sequence alignments to rationally perturb E2-E6AP binding preferences.

Results

E6AP selectivity for Ubch7 and Ubch8

Previous two-hybrid studies and activity assays indicate that E6AP binds and functions with the E2s Ubch7 and Ubch8, and to a lesser extent Ubch5a^{19; 20}. To more precisely quantitate these preferences and test a larger set of E2s, we measured the binding affinity of E6AP for 9 E2s using a fluorescence polarization (FP) assay that we previously used to measure Ubch7-E6AP binding²³. E2s were selectively labeled at cysteine side-chains using a thiol-reactive bodipy dye, and fluorescence polarization of the modified E2 was monitored as a function of E3 concentration. To ensure that the bodipy labeling of the E2s was not influencing binding, we measured the binding affinity of unmodified Ubch7 for E6AP using isothermal titration calorimetry (ITC) (Supplementary Figure 1). The two experiments yielded similar measures of the Ubch7-E6AP dissociation constant (K_D of 5.0 M from FP and 2.2 M from ITC). Of the E2s tested only Ubch8 contained a cysteine near the HECT-binding interface and for this reason we used a C97S Ubch8 mutant in our FP assays.

Four of the E2s (Ubch9, Ubch10, Rad6b, and Ubch12) lack a phenylalanine at position 63 (F63) and were not expected to bind E6AP (Figure 2(a)). The E2s with a F63 represent three distinct E2 subfamilies according to a recent phylogenetic analysis of E2 enzymes²⁴. Representatives of the UBC4/5 subfamily include yeast UBC4 and its human homolog Ubch5b (Ubch5a paralog). The human Ubch2 protein belongs to the UBC8 subfamily while human Ubch7 and Ubch8 represent the Ubch7/8 subfamily. The binding assays show that only Ubch7 and Ubch8(C97S) bind to E6AP with low micromolar affinity (Figure 2(b)). The other E2s with a phenylalanine at position 63 (UBC4, Ubch5b, and Ubch2) bind E6AP with affinities less than 200 M. Of the E2s lacking F63, Ubch10, Rad6b, and Ubch12 did not bind E6AP. Ubch9, the SUMO-conjugating enzyme, was able to weakly interact with E6AP. These results are consistent with previous findings that show HECT E3s preferentially interact with E2s containing a phenylalanine at position 63^{11; 18}.

Identifying hot spot residues at the Ubch7–E6AP interface

Having confirmed the importance of F63 to binding E6AP, we next set out to identify secondary determinants that provide E6AP selectivity for the Ubch7/8 subfamily. We used alanine scanning of the E6AP-Ubch7 interface followed by binding measurements to determine which side chains contribute most to binding. 36 residues at the interface were mutated to either alanine or glycine. The mutants were expressed in *E. coli*. and binding affinities were measured with the FP binding assay.

The free energy of binding for the wild type Ubch7–E6AP interaction was measured at 7.2 kcal/mol ($K_D = 5.0$ M). As expected, the mutation resulting in the largest loss of binding energy was F63A ($\Delta\Delta G^\circ_{bind} = 3.0$ kcal/mol). None of the other mutants tested lost more than 2 kcal/mol, but 9 mutants lost greater than 1 kcal/mol. Together with F63 these residues will be referred to as hot spots (Table 1). Of these 9 mutants, 4 are hydrophobic E6AP residues (L635A, L639A, L642A, and F690A) that form van der Waals contacts with F63 (Figure 3). An unexpected finding was that two Ubch7 loop 7 lysine residues, K96 and K100, were binding hot spots. In the crystal structure, K96 forms a salt bridge with D641 of E6AP while the K100 hydrogen bonds with the D652 backbone carbonyl of E6AP. Hot spots were also observed at a completely conserved proline preceding F63 as well as M653 and Y645 of E6AP. The latter two residues form van der Waals contacts with P97 and A98 of Ubch7 loop 7. Of the remaining mutants we found 16 to be moderately destabilizing ($\Delta\Delta G^\circ_{bind}$ of 0.25 to 1.0 kcal/mol). These residues are a mixture of polar, charged, and hydrophobic amino acids. Interestingly these residues form a shell around the hydrophobic hot spot residues of Ubch7 and E6AP (Figure 3). Like the reciprocating hydrophobic hot spots, moderately destabilizing residues of Ubch7

interact with moderately destabilizing residues of E6AP. The final 10 mutants exhibited either neutral ($\Delta\Delta G^{\circ}_{bind}$ of -0.25 to 0.25 kcal/mol) or stabilizing ($\Delta\Delta G^{\circ}_{bind} < -0.25$ kcal/mol) effects on the binding free energy. These residues cluster further from the hot spots and outside the shell of moderately destabilizing residues (Figure 3). The observed pattern of an energetically important hydrophobic interface core surrounded by a shell of energetically less important residues is not uncommon to protein–protein interfaces^{25; 26}.

Other mutations were made to UbcH7 and E6AP to serve as controls. In the UbcH7–E6AP crystal structure, R52 of UbcH7 is solvent exposed and situated opposite the binding interface. Mutation of this residue to alanine resulted in wild type binding affinity (Table 1). Similarly, no change in binding free energy was observed upon mutating the E6AP catalytic cysteine to alanine (C820A) (Table 1). Previous studies on the WWP1 HECT domain found that a double proline mutation in the hinge connecting the N and C lobes resulted in reduced ligase activity¹². To confirm that the impaired activity arises from restricted conformational flexibility and not perturbed binding, the analogous positions in E6AP were mutated to prolines (S739P N741P). The resulting mutant bound UbcH7 with wild type affinity (Table 1).

Charge swap mutations at the UbcH7–E6AP interface

To identify charged amino acids engaged in electrostatic interactions across the interface we measured binding affinities of 10 UbcH7–E6AP charge swap mutants (Table 1). The binding affinities from the charge swap experiments were grouped into the same categories as the alanine mutant affinities. Six of the mutants lost > 1.0 kcal/mol of binding free energy. These include UbcH7 helix 1 mutants R5E, R6E, and K9E as well as loop 7 charge swaps K96E and K100E. The helix 1 mutants form inter-chain (R5 and R6) and intra-chain (K9) hydrogen bonds to backbone oxygen atoms. The D652R mutation was also largely destabilizing, possibly because of a loss of interaction with K100. Three of the remaining charge swap mutants displayed less significant losses in binding energy (E60R, K64E, and D641K). The E93R mutant displayed a large gain in binding energy that may be the result of a new hydrogen bond with the Q637 E6AP side chain.

Only two side chain–side chain charged interactions are present across the interface, K100–D652 and K96–D641. We proceeded to test the mutant pairs for an altered specificity interaction. The effects from K100E–D652R interaction were as unfavorable as the effects of either single mutant ($\Delta\Delta G_{bind}$ of 1.6 kcal/mol). In contrast, the K96E–D641K mutant pair displayed a charge swap interaction that was more favorable than the wild type interaction ($\Delta\Delta G_{bind}$ of -0.8 kcal/mol). For the purpose of creating an altered specificity UbcH7–E6AP pair, the K96–D641K mutant pair would only achieve specificity towards E3s because the D641K mutant displays no defects in binding wild type UbcH7. A sub-optimal K96–D641K salt bridge in the wild type interaction could give rise to such results. These findings suggest that creating an altered specificity UbcH7–E6AP pair using a charge swap interaction may prove difficult.

Ubiquitin transfer rates correlate with UbcH7-E6AP binding affinity

Ubiquitin transfer assays were used to assess if changes in UbcH7–E6AP binding affinity influence the rate ubiquitin is transferred to E6AP. Activity assays were not performed with mutant UbcH7 proteins because of potential complications from altered E1-UbcH7 activity. All E6AP mutants were tested in reactions containing radiolabeled ubiquitin, E1, UbcH7, ATP and an ATP regenerating system. Each reaction was quenched in SDS-PAGE loading buffer lacking β -ME, separated by SDS-PAGE, and ubiquitin-modified proteins were visualized using a phosphorimager (Figure 4(a)). Ubiquitin-modified E6AP appears as two bands and UbcH7 as a single band. The wild type reaction quenched in loading buffer containing β -ME demonstrates that the ubiquitin modifications to both UbcH7 and the faster migrating E6AP

band are mediated via thioester linkages (denoted with ~). The slower migrating E6AP band that is resistant to treatment with β -ME likely represents ubiquitin modification via an isopeptide bond (denoted with -). No ubiquitin-modified E6AP is observed in reactions using the catalytic cysteine mutant (C820A) or the control lacking E6AP.

Phosphoimaging software was used to quantitate the total amount of Ub~E6AP formed in each reaction as well as the amount of Ub~UbcH7 (Figure 4(b)). Ub-UbcH7 levels were not constant between the various reactions indicating that the rates of Ub~E6AP formation were partially limited by the E1/UbcH7 reaction rates. Indeed, in reactions with the tighter binding E2-E3 pairs the Ub~UbcH7 band was very weak suggesting that the rate of Ub~E6AP formation depended almost entirely on the E1/UbcH7 reaction rate. Previously, we have shown that E3 and E1 binding to UbcH7 are mutually exclusive and that saturating amounts of E3 can inhibit the E1/E2 transfer step²³. We do not believe that is occurring in this case as the E3 concentrations are well below saturating levels. Despite being partially limited by the E1/E2 transfer step, there is still a correlation between the amount of Ub~E6AP formed and the E2/E3 binding affinities (correlation coefficient = 0.58). E6AP hot spot mutants Y645A, D652R, F690A, and M653A as well as Y694L, M654A, and S739P N741P formed less than 55% of the ubiquitin-E6AP observed in the wild type reactions. All the E6AP mutants displaying enhanced binding affinity resulted in an increase in the formation of ubiquitin-E6AP. There are a few outliers. L639A and L635A weaken binding by > 1 kcal / mol, but do not show a reduced amount of Ub~E6AP formed. However, there is a greater build up of Ub~UbcH7 for these two reactions than for the wild type reaction. Overall, the results indicate that E2/E3 binding affinity does affect E2/E3 ubiquitin transfer rates, but that there could be additional important factors such as on and off rates, rate of transfer within the bound complex and the affinity of ubiquitin charged E2 for the E3.

UbcH7–E6AP hot spots are essentially conserved in the UbcH8–E6AP interaction

The hot spot residues in UbcH7, F63, K96 and K100, are conserved in UbcH8 (F62, K95 and K99). To confirm that these residues are playing the same role at the UbcH8–E6AP interface we mutated them to alanine and measured affinity for E6AP. The UbcH8 F62A mutation abolished binding to E6AP. The K95A and K99A mutations proved to be destabilizing with losses in binding energy of 0.9 and 1.3 kcal/mol respectively (Table 2). In both E2s, the double loop 7 mutants show nearly additive effects from the single mutants, but still the combined destabilization is less than the loop 4 phenylalanine mutation. We also tested our panel of E6AP mutants with UbcH8 in binding assays. There is a striking similarity in the binding affinities of UbcH7 and UbcH8 for E6AP mutants (Figure 5). Only two significant discrepancies are observed and these are L639A and D641K; both are stabilizing with UbcH8 yet destabilizing with UbcH7. These results show that hot spots at the UbcH7–E6AP interface are also hot spots at the UbcH8–E6AP interface.

Redesigning UbcH5b to bind E6AP

To further explore the determinants of E2-E6AP binding specificity we characterized a set of mutations that were rationally designed to induce UbcH5b to bind more tightly to E6AP. Our first design strategy was to mutate residues in UbcH5b that map to hot spot positions in UbcH7. We made the S94K and T98K single and double mutants in UbcH5b and measured binding to E6AP (Figure 6). The S94K mutant destabilized binding by 0.5 kcal/mol while the T98K strengthened binding by 0.4 kcal/mol. The double mutant bound weaker than wild type UbcH5b but stronger than the S94K single mutant. A possible explanation for this result is that the extra residue present in UbcH7/8 loop 7 (Figure 2(a)) may lead to different loop 7–E6AP interactions in UbcH5b. From these results it is clear that conserving the hot spot residues from UbcH7 is not sufficient to induce low micromolar binding with E6AP.

To further search for UbcH5b mutations that could increase affinity for E6AP we examined the E2 multiple sequence alignment for residues that were not conserved between UbcH7 and UbcH5b but were located at the E6AP–UbcH7 interface. The only residue that differs between the proteins and had an affect on UbcH7–E6AP affinity is serine 4 on UbcH7, which is a leucine in UbcH5b. Somewhat surprisingly, mutating this leucine on UbcH5b to serine (L3S) resulted in a significant gain of 1.2 kcal/mol in binding energy (K_D of 23 M) (Figure 6). This mutation was tested in conjunction with the S94K and T98K mutants mentioned above, and the L3S T98K double mutant bound E6AP with UbcH7/8-like affinity. So although the serine at residue 4 in UbcH7 is not making strong favorable interactions with E6AP, the residue located at this position can have a significant impact on E2-E6AP binding specificity. The leucine at this position in UbcH5b is dictating specificity by disfavoring interactions with E6AP.

Discussion

The sequence determinants of E2-E6AP binding affinity and specificity have been studied by mutational analysis. The major findings can be summarized as follows. (1) a F63 in loop 4 of an E2 is necessary but not sufficient for tight E2–E6AP binding affinity as the 5 E2s that were characterized with this phenylalanine bind with affinities ranging from 5–180 M. Of these E2s only UbcH7 and UbcH8 bind E6AP with low micromolar affinity. (2) In addition to F63, three side chains on UbcH7 contribute > 1 kcal/mol to the binding free energy between UbcH7 and E6AP. Two of these (K96 and K100) are located on the periphery of the interface and are not conserved in other E2 subfamilies that bind more weakly to E6AP. (3) The E6AP side chains that contribute most to binding UbcH7 are hydrophobic and surround the F63 binding cleft. (4) Residues that are not hot spots for the UbcH7-E6AP interaction can contribute significantly to E2-E6AP binding specificity. Mutating L3 of UbcH5b to a serine led to a ~10 fold increase in UbcH5b-E6AP affinity.

An important question that remains is whether the interactions that determine E6AP-E2 specificity will translate to other E2-HECT interfaces. Much of the initial work on E2-HECT specificity focused on E6AP and *S. cerevisiae* Rsp5. Different techniques yielded conflicting results as to which E2s these E3s preferred. Studies using the yeast two-hybrid method showed that E6AP selectively interacts with UbcH7 and UbcH8 while Rsp5 prefers UbcH5a and UbcH6²⁰. Other results using substrate or E3 ubiquitination assays show that UbcH5a and UbcH7 support equal E6AP activity or that Rsp5 is not active with UbcH6^{18; 19; 22}. One consistent finding was that Rsp5 prefers UbcH5a. Many human HECT E3s are closely related to yeast Rsp5 in their HECT domain as well as N-terminal substrate binding domains (Nedd4, Nedd4L, Smurf1/2, WWP1/2 and AIP4 in humans)²⁷. A sequence alignment of the E2 binding region of HECT E3s (Figure 7) shows that within the Rsp5 subfamily there are conserved residues not present in E6AP. Some of these differences map to a loop that is 1-3 residues shorter than E6AP in the Rsp5 subfamily. In more structurally defined positions notable differences are observed at E6AP residues D641 (W in Rsp5 subfamily), V634 (D/E), and Y645 (N), and F690 (Y). In an attempt to optimize the UbcH7–Smurf2 interaction, Ogunjimi et al found two mutations to Smurf2 that were capable of enhancing catalytic activity *in vitro* and *in vivo*¹³. These mutations, H547I and Y581F, replaced polar groups in the binding groove with hydrophobic residues observed in E6AP (I655 and F690). Other Rsp5 family members maintain the hydrophobic nature of I655. Whether subtle differences within other Rsp5 family members will drive specificity towards the UBC4/5 family or towards other E2 families with a F63 remains undetermined. Our results show that a subtle difference between UBC4 and UbcH5b indeed affects binding to E6AP.

Our *in vitro* ubiquitination assays with E6AP mutants demonstrate that E2-E3 affinity influences the rate ubiquitin~HECT thioesters can be formed. *In vivo* there will be the added complexity that a variety of E3s will be competing for E2 binding sites which could make E3

conjugation rates more sensitive to E2-E3 affinity. Additionally, the study by Ogunjimi et al. found that an auxiliary protein Smad7 was able to bind both UbcH7 and the Smurf2 E3 via its WW domain and effectively enhance the activity of Smurf2¹³. This finding suggests that in some cases the specificity of E2-E3 interactions may reside in a tertiary protein. Discovering which E2-E3 pairs functionally interact in the cell is a challenging problem. Introducing E2s and E3s with redesigned binding specificities into the cell may provide one route for deciphering the importance of specific interactions. Our study (and others like it) on the determinants of E2-E3 specificity lay the foundation for such efforts.

Materials and Methods

Protein Purification

UbcH7, ubiquitin, and E6AP expression plasmids have been previously described²³. All other clones were obtained in or subcloned into pGEX vectors with N-terminal GST-tags followed by a thrombin recognition sequence. Vectors harboring *S. cerevisiae* UBC4 and human UbcH5b, UbcH8, UbcH10, Rad6b, and UbcH2 were kindly provided by Marc Timmers. Human Ubc12 and Ubc9 were kindly provided by Brenda Schulman and Jon Huibgretse respectively. Point mutations were introduced using the QuickChange® sitedirected mutagenesis protocol (Stratagene). All vectors were verified by DNA sequencing.

Proteins were expressed overnight at 25 °C with 0.3 mM IPTG in the BL21(DE3) strain of *E. coli*. Cells were disrupted by sonication and the resulting lysates were cleared by ultracentrifugation. UbcH7 was purified by metal chelating sepharose followed by cation exchange and gel filtration. Ubiquitin was purified by metal chelating sepharose followed by thrombin cleavage and gel filtration. The HECT domain of E6AP and all other E2s were purified by glutathione sepharose followed by thrombin cleavage, anion exchange and gel filtration. For the Y694A E6AP mutant we were not able to purify a sufficient amount of protein, so instead we tested the Y694L mutation. Proteins were concentrated using Centricon® and Centriprep® centrifugal concentrators. Extinction coefficients used to determine protein concentrations were calculated using the method of Gill and von Hippel²⁸.

Isothermal Titration Calorimetry Binding Assay

A Microcal-VP-ITC was used to measure the binding thermodynamics of unmodified UbcH7 for E6AP (Supplementary Figure 1). The experiment was performed at 25° C using 700 M UbcH7 in the sample syringe and 1.45 mL of 35 M E6AP in the sample cell. Forty-one 5 L injections of UbcH7 were performed at 5 minute intervals. The heat of dilution of UbcH7 was calculated as the average of the final three titrations and this value was subtracted from the dataset. Origin software was used to fit the data to a single-site binding model and determine the stoichiometry (N) and thermodynamic parameters of binding ΔH_{bind} , ΔG_{bind} and ΔS_{bind} .

Fluorescence Polarization Binding Assays

Binding assays, data analysis, and labeling of the E2 enzymes with bodipy (507/545)-iodoacetamide (Molecular Probes) has been previously described²³. Starting concentrations for bodipy-E2 depended on the extent of conjugated fluorophore and typically fell in the range of 0.5-2.0 M. Manual titrations were performed using wild type and mutant E6AP(HECT) stock solutions that varied based on yield and strength of the interaction. All binding assays were performed at room temperature in 20 mM KH₂PO₄ pH 7.0, 150 mM NaCl and 5 mM β -mercaptoethanol (β -ME). For each binding experiment, nine polarization readings were collected and averaged at twenty concentrations of E6AP(HECT). Data was fit to a single-site binding model using nonlinear regression with SigmaPlot software to yield parameters for P_{min} (starting polarization), P_{max} (maximum polarization), and K_D (dissociation constant).

***In Vitro* Ubiquitin Transfer Assay**

Isotopic labeling of ubiquitin with ^{32}P was carried out using the PKAce™ kit (Novagen) according to the manufacturer's protocol. The labeling reaction was quenched with a 10-fold molar excess of protein kinase A inhibitor (PKI 6-22 Amide, EMD Biosciences). Assays were carried out at 4 °C for 20 minutes in 50 L volumes containing 20 mM Tris pH 7.5, 50 mM NaCl, 10 mM MgCl₂, 0.2 mM β-ME, 2 mM ATP, 10 mM creatine phosphate, 10 U/ml creatine kinase, 5 M ^{32}P -ubiquitin, 50 nM human E1 (Boston Biochem), 1 M Ubch7, and 1 M wild type or mutant E6AP(HECT). Reactions were initiated with the addition of ^{32}P -ubiquitin and terminated with 2X SDS-PAGE loading buffer with or without 200 mM β-ME. SDS-PAGE was used to separate 30 L of the final reactions and gels were then dried and exposed to a phosphor screen. A phosphorimager and ImageQuant 5.0 software (GE Healthcare) were used to detect and quantify ^{32}P -ubiquitin bands. The experiment was performed in duplicate (Supplementary Figure 2).

Supplementary Material

Refer to Web version on PubMed Central for supplementary material.

References

1. Hershko A, Ciechanover A. The ubiquitin system. *Annu Rev Biochem* 1998;67:425–79. [PubMed: 9759494]
2. Scheffner M, Nuber U, Huibregtse JM. Protein ubiquitination involving an E1-E2-E3 enzyme ubiquitin thioester cascade. *Nature* 1995;373:81–3. [PubMed: 7800044]
3. Schwartz AL, Ciechanover A. The ubiquitin-proteasome pathway and pathogenesis of human diseases. *Annu Rev Med* 1999;50:57–74. [PubMed: 10073263]
4. Glickman MH, Ciechanover A. The ubiquitin-proteasome proteolytic pathway: destruction for the sake of construction. *Physiol Rev* 2002;82:373–428. [PubMed: 11917093]
5. Winkler GS, Albert TK, Dominguez C, Legtenberg YI, Boelens R, Timmers HT. An altered-specificity ubiquitin-conjugating enzyme/ubiquitin-protein ligase pair. *J Mol Biol* 2004;337:157–65. [PubMed: 15001359]
6. Martinez-Noel G, Muller U, Harbers K. Identification of molecular determinants required for interaction of ubiquitin-conjugating enzymes and RING finger proteins. *Eur J Biochem* 2001;268:5912–9. [PubMed: 11722579]
7. Zheng N, Schulman BA, Song L, Miller JJ, Jeffrey PD, Wang P, Chu C, Koepf DM, Elledge SJ, Pagano M, Conaway RC, Conaway JW, Harper JW, Pavletich NP. Structure of the Cul1-Rbx1-Skp1-F boxSkp2 SCF ubiquitin ligase complex. *Nature* 2002;416:703–9. [PubMed: 11961546]
8. Ulrich HD. Protein-protein interactions within an E2-RING finger complex. Implications for ubiquitin-dependent DNA damage repair. *J Biol Chem* 2003;278:7051–8. [PubMed: 12496280]
9. Katoh S, Tsunoda Y, Murata K, Minami E, Katoh E. Active site residues and amino acid specificity of the ubiquitin carrier protein-binding RING-H2 finger domain. *J Biol Chem* 2005;280:41015–24. [PubMed: 16186120]
10. Scheffner M, Huibregtse JM, Vierstra RD, Howley PM. The HPV-16 E6 and E6-AP complex functions as a ubiquitin-protein ligase in the ubiquitination of p53. *Cell* 1993;75:495–505. [PubMed: 8221889]
11. Huang L, Kinnucan E, Wang G, Beaudenon S, Howley PM, Huibregtse JM, Pavletich NP. Structure of an E6AP-UbcH7 complex: insights into ubiquitination by the E2-E3 enzyme cascade. *Science* 1999;286:1321–6. [PubMed: 10558980]
12. Verdecia MA, Joazeiro CA, Wells NJ, Ferrer JL, Bowman ME, Hunter T, Noel JP. Conformational flexibility underlies ubiquitin ligation mediated by the WWP1 HECT domain E3 ligase. *Mol Cell* 2003;11:249–59. [PubMed: 12535537]

13. Ogunjimi AA, Briant DJ, Pece-Barbara N, Le Roy C, Di Guglielmo GM, Kavsak P, Rasmussen RK, Seet BT, Sicheri F, Wrana JL. Regulation of Smurf2 ubiquitin ligase activity by anchoring the E2 to the HECT domain. *Mol Cell* 2005;19:297–308. [PubMed: 16061177]
14. Nawaz Z, Lonard DM, Smith CL, Lev-Lehman E, Tsai SY, Tsai MJ, O'Malley BW. The Angelman syndrome-associated protein, E6-AP, is a coactivator for the nuclear hormone receptor superfamily. *Mol Cell Biol* 1999;19:1182–9. [PubMed: 9891052]
15. Cooper EM, Hudson AW, Amos J, Wagstaff J, Howley PM. Biochemical analysis of Angelman syndrome-associated mutations in the E3 ubiquitin ligase E6-associated protein. *J Biol Chem* 2004;279:41208–17. [PubMed: 15263005]
16. Pickart CM. Mechanisms underlying ubiquitination. *Annu Rev Biochem* 2001;70:503–33. [PubMed: 11395416]
17. Zheng N, Wang P, Jeffrey PD, Pavletich NP. Structure of a cCbl-UbcH7 complex: RING domain function in ubiquitin-protein ligases. *Cell* 2000;102:533–9. [PubMed: 10966114]
18. Nuber U, Scheffner M. Identification of determinants in E2 ubiquitinconjugating enzymes required for hect E3 ubiquitin-protein ligase interaction. *J Biol Chem* 1999;274:7576–82. [PubMed: 10066826]
19. Nuber U, Schwarz S, Kaiser P, Schneider R, Scheffner M. Cloning of human ubiquitin-conjugating enzymes UbcH6 and UbcH7 (E2-F1) and characterization of their interaction with E6-AP and RSP5. *J Biol Chem* 1996;271:2795–800. [PubMed: 8576257]
20. Kumar S, Kao WH, Howley PM. Physical interaction between specific E2 and Hect E3 enzymes determines functional cooperativity. *J Biol Chem* 1997;272:13548–54. [PubMed: 9153201]
21. Anan T, Nagata Y, Koga H, Honda Y, Yabuki N, Miyamoto C, Kuwano A, Matsuda I, Endo F, Saya H, Nakao M. Human ubiquitin-protein ligase Nedd4: expression, subcellular localization and selective interaction with ubiquitin-conjugating enzymes. *Genes Cells* 1998;3:751–63. [PubMed: 9990509]
22. Schwarz SE, Rosa JL, Scheffner M. Characterization of human hect domain family members and their interaction with UbcH5 and UbcH7. *J Biol Chem* 1998;273:12148–54. [PubMed: 9575161]
23. Eletr ZM, Huang DT, Duda DM, Schulman BA, Kuhlman B. E2 conjugating enzymes must disengage from their E1 enzymes before E3-dependent ubiquitin and ubiquitin-like transfer. *Nat Struct Mol Biol* 2005;12:933–4. [PubMed: 16142244]
24. Winn PJ, Religa TL, Battey JN, Banerjee A, Wade RC. Determinants of functionality in the ubiquitin conjugating enzyme family. *Structure* 2004;12:1563–74. [PubMed: 15341722]
25. Clackson T, Wells JA. A hot spot of binding energy in a hormone receptor interface. *Science* 1995;267:383–6. [PubMed: 7529940]
26. Bogan AA, Thorn KS. Anatomy of hot spots in protein interfaces. *J Mol Biol* 1998;280:1–9. [PubMed: 9653027]
27. Ingham RJ, Gish G, Pawson T. The Nedd4 family of E3 ubiquitin ligases: functional diversity within a common modular architecture. *Oncogene* 2004;23:1972–84. [PubMed: 15021885]
28. Gill SC, von Hippel PH. Calculation of protein extinction coefficients from amino acid sequence data. *Anal Biochem* 1989;182:319–26. [PubMed: 2610349]

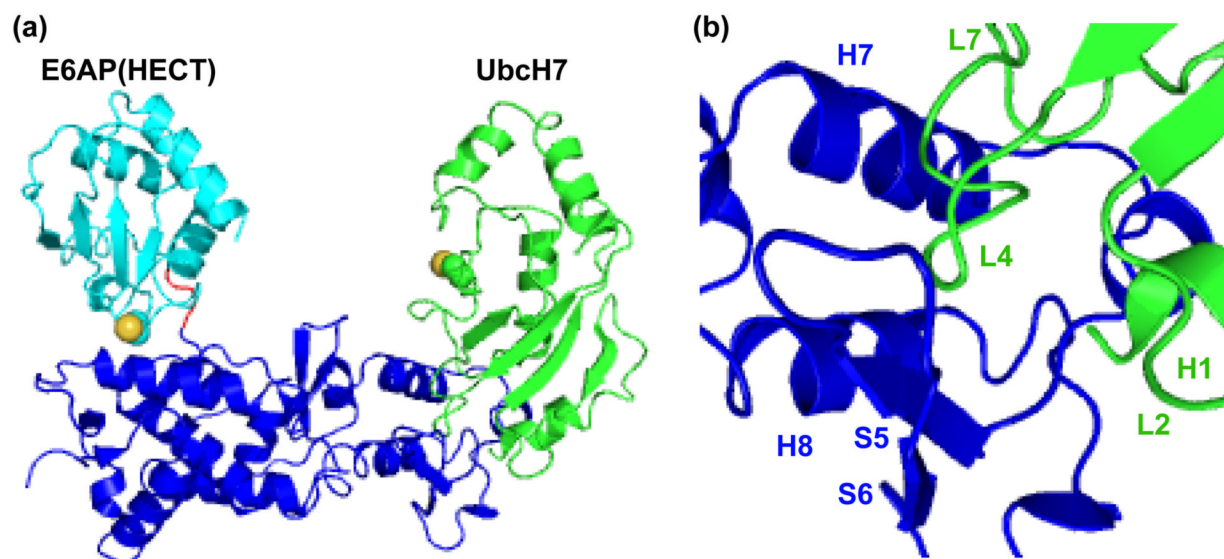


Figure 1.

Cartoon representation of the Ubch7–E6AP crystal structure¹¹. (a) The E6AP N-terminal lobe (blue) and C-terminal lobe (cyan) are connected by a 3 residue hinge (red). E6AP uses a ~80 amino acid subdomain in the N-terminal lobe to bind Ubch7 (green). Catalytic cysteine side chains of Ubch7 and E6AP are shown as van der Waals radii. (b) Close up of the Ubch7–E6AP interface. The most significant contacts arise from Ubch7 helix 1 (H1) as well as loops 4 and 7 (L4 and L7) which interact with E6AP helices 7 and 8 (H7 and H8) and the H7-S5 loop. Figure was generated using PDB 1C4Z¹¹ and PYMOL (<http://www.pymol.org>).

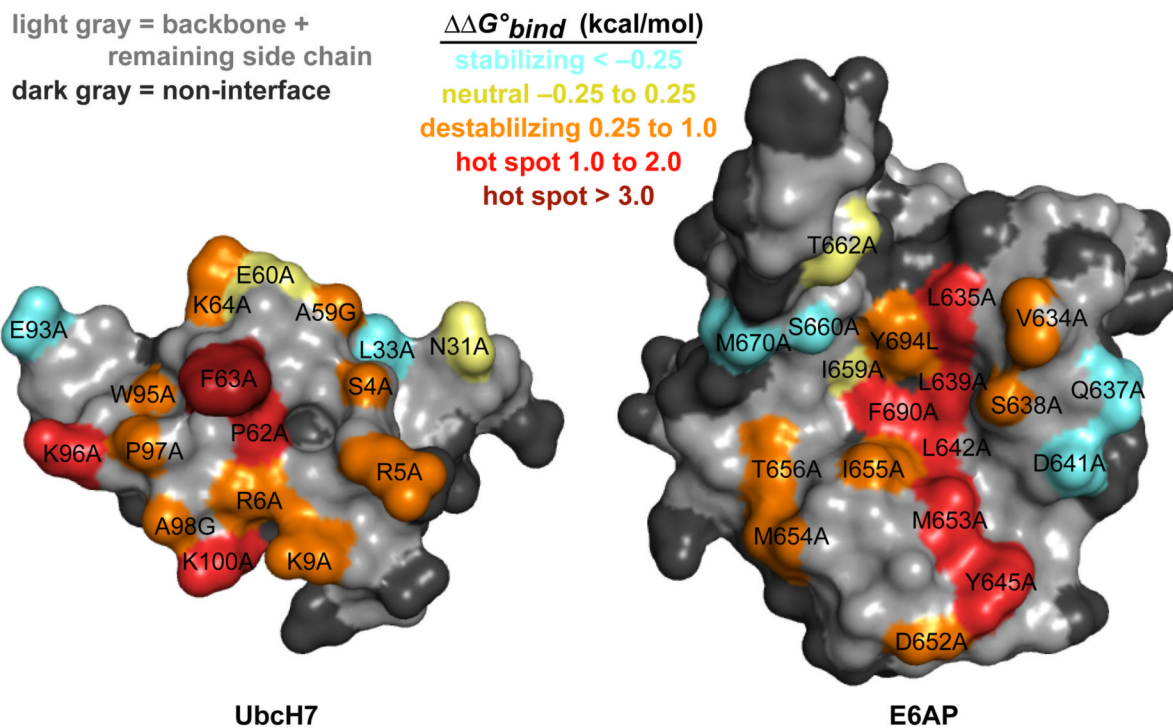


Figure 3. Mapping $\Delta\Delta G_{bind}$ from alanine scan studies onto the UbH7-E6AP structure. The interface view was obtained by rotating UbH7 180° about the y-axis. Individual amino acids are colored by the change in binding free energy observed upon making the indicated mutation. F63 of UbH7 is the most important residue for binding. Other hot spots include E6AP residues lining the hydrophobic groove that contacts F63 as well as K96 and K100 of UbH7. Residues with smaller contributions to binding form a shell around F63 and the hydrophobic E6AP groove. Figure was generated using PDB 1C4Z¹¹ and PYMOL.

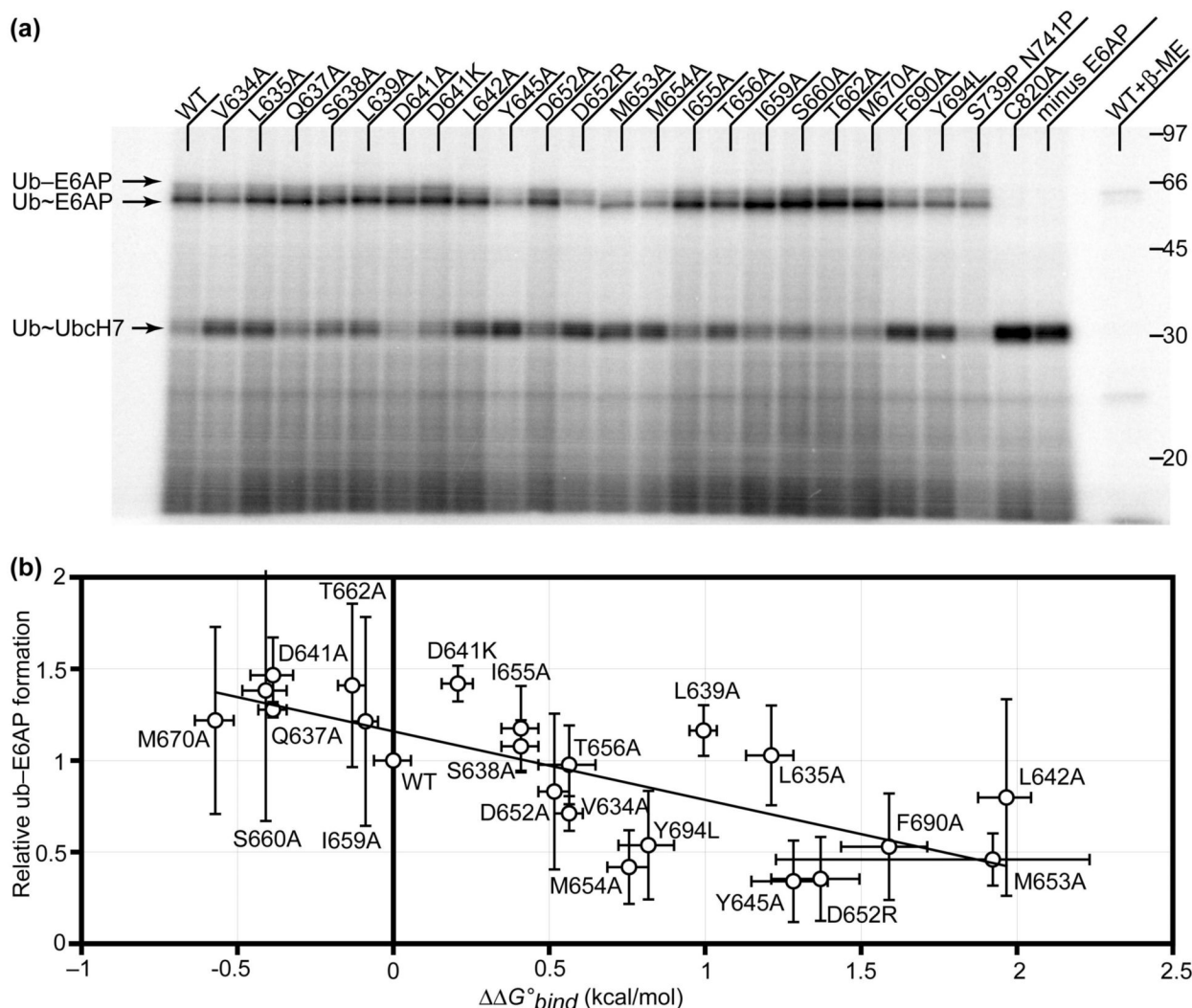


Figure 4. *In vitro* activity of E6AP mutant proteins. (a) A ubiquitin transfer assay was used to detect the formation of ubiquitin-E6AP thioester in reactions containing 5 M ³²P-ubiquitin, 50 nM E1, 1 M wild type UbcH7 and 1 M wild type or mutant E6AP and an ATP regenerating buffer. The ubiquitin-E6AP thioester (Ub~E6AP) is reduced in the control reaction quenched in β-ME while the isopeptide-linked ubiquitin (Ub-E6AP) is retained. (b) For each reaction the total ubiquitin-E6AP formed was quantified and normalized to the wild type reaction. The assay was repeated (Supplementary Figure 1) and the averaged counts for each mutant is plotted versus the experimentally determined ΔΔG°*bind*. Error bars represent standard deviation of relative ub-E6AP formed and the standard error of ΔΔG°*bind*.

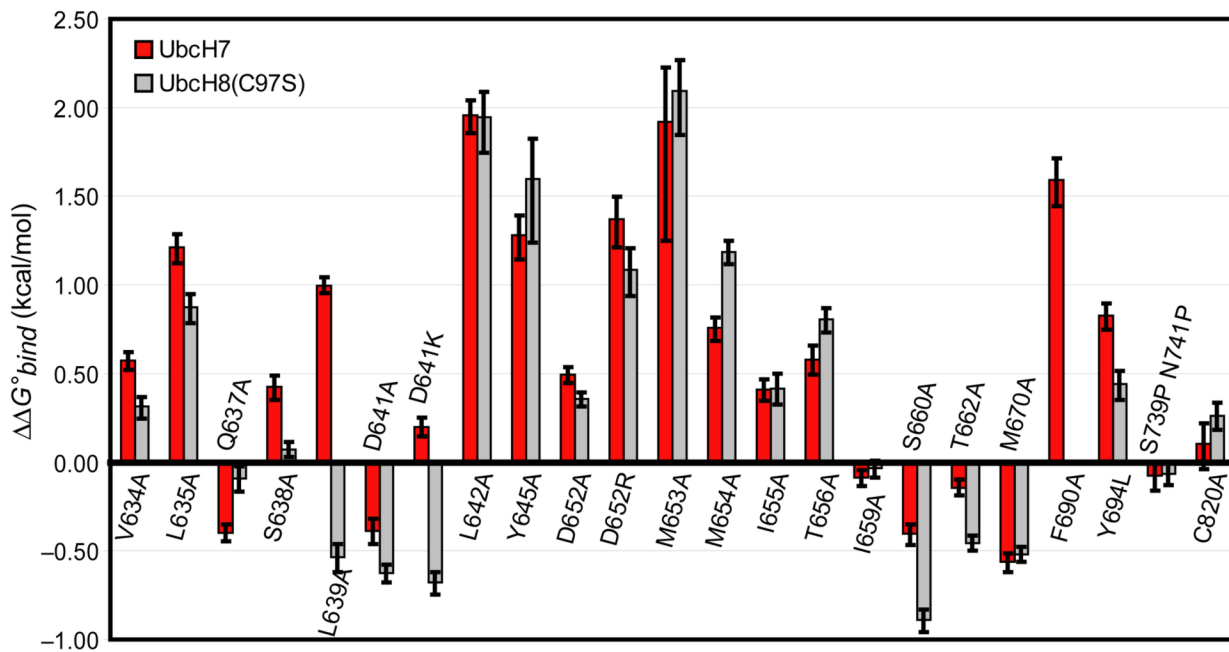


Figure 5. Ubch7 and Ubch8 form nearly identical interactions with E6AP. Bar graph comparing the observed change in binding free energy of E6AP mutants for Ubch7 and Ubch8(C97S). Nearly all E6AP interface residues contribute similar energy to binding Ubch7 and Ubch8(C97S). The two significant differences (L639A and the charge swap D641K) may arise from a slight difference in loop L7 of Ubch7 and Ubch8. The F690A mutant was not tested with Ubch8.

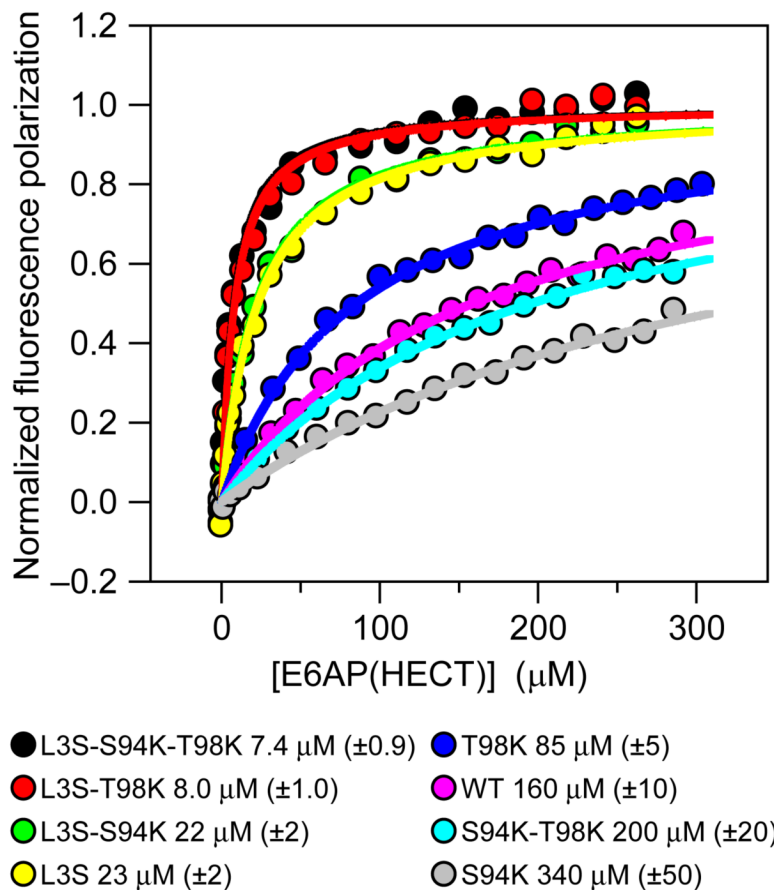


Figure 6. Rationally manipulating UbcH5b to enhance binding to E6AP. Three UbcH5b positions were mutated and tested for their contribution to binding E6AP. UbcH5b mutants containing the UbcH7 hot spot lysine(s) (S94K and T98K) alone were not able to significantly enhance binding. The L3 UbcH5b residue is a serine in UBC4, UbcH7 and UbcH8, and the L3S mutation resulted in a large increase in binding affinity for E6AP. The L3S T98K double mutant was capable of binding E6AP with UbcH7/8-like affinity. Interestingly the S94K mutation is destabilizing except when present with the L3S mutation.

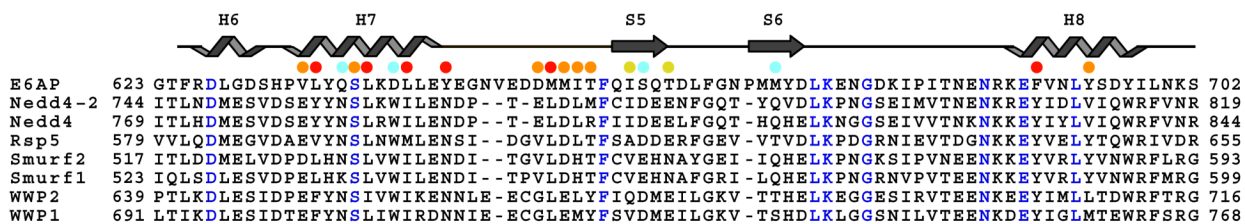


Figure 7. Multiple sequence alignment of the E2-binding subdomain of Rsp5 family members and E6AP. The dots are colored by the change in UbH7-E6AP binding energy associated with mutating the E6AP side chain to alanine according to Figure 3. Amino acids lining the hydrophobic groove that interacts with F63 of E2s is generally hydrophobic and/or aromatic in the Rsp5 family of E3s. The Rsp5 family members have a 1-3 residue deletion in the H7-S5 loop and numerous non-conservative substitutions at E6AP residues. Both of these differences likely play a role in dictating E2-HECT specificity.

Table 1

Measured dissociation constants for UbcH7 and E6AP(HECT) mutants

UbcH7	K_D (M)	$\Delta\Delta G^*_{bind}$ (kcal/mol)	E6AP	K_D (M)	$\Delta\Delta G^*_{bind}$ (kcal/mol)
WT	5.0 ± 0.5	0	WT	5.0 ± 0.5	0
S4A	13 ± 1	0.54	Y634A	13 ± 1	0.57
R5A	12 ± 2	0.51	L635A	39 ± 5	1.2
R5E	44 ± 10	1.3	Q637A	2.6 ± 0.2	-0.40
R6A	11 ± 2	0.46	S638A	10 ± 1	0.42
R6E	37 ± 8	1.2	L639A	27 ± 2	1.0
K9A	14 ± 2	0.62	D641A	2.6 ± 0.3	-0.39
K9E	69 ± 22	1.6	D641K	7.1 ± 0.6	0.20
N31A	3.7 ± 0.3	-0.18	L642A	140 ± 20	2.0
L33A	2.8 ± 0.7	-0.36	Y645A	44 ± 9	1.3
R52A	4.9 ± 0.5	-0.02	D652A	12 ± 1	0.49
A59G	13 ± 2	0.54	D652R	51 ± 12	1.4
E60A	5.8 ± 0.7	0.09	M653A	130 ± 90	1.9
E60R	5.6 ± 1.2	0.06	M654A	18 ± 2	0.76
P62A	54 ± 10	1.4	I655A	10 ± 1	0.41
F63A	810 ± 550	3.0	T656A	13 ± 2	0.58
K64A	8.2 ± 1.1	0.29	I659A	4.3 ± 0.3	-0.09
K64E	17 ± 3	0.71	S660A	2.5 ± 0.3	-0.41
E93A	2.4 ± 0.3	-0.43	T662A	4.0 ± 0.3	-0.14
E93R	0.92 ± 0.09	-1.0	M670A	1.9 ± 0.2	-0.56
W95A	20 ± 2	0.83	F690A	74 ± 17	1.6
K96A	34 ± 6	1.1	Y694L	20 ± 3	0.83
K96E	36 ± 13	1.2	S739P N741P	4.4 ± 0.6	-0.07
P97A	21 ± 2	0.85	C820A	6.0 ± 1.3	0.10
A98G	10 ± 1	0.41			
K100A	45 ± 15	1.3			
K100E	55 ± 26	1.4			

Table 2
Measured $\Delta\Delta G_{bind}$ (kcal/mol) of UbCH7–E6AP hot spots in UbCH8(C97S)

	UbCH7		UbCH8(C97S)
F63A	3.0	F62A	DNB
K96A	1.1	K95A	0.9
K100A	1.3	K99A	1.3
K96A K100A	2.1	K95A K99A	2.1

DNB, does not bind in our assay.